Received March 22, 2017, accepted April 14, 2017, date of publication May 2, 2017, date of current version June 28, 2017.

Digital Object Identifier 10.1109/ACCESS.2017.2700474

Vegetation Index Differencing for Estimating Foliar Dust in an Ultra-Low-Grade Magnetite Mining Area Using Landsat Imagery

BAODONG MA[1,2,3], RUILIANG PU[3], LIXIN WU[1,2], AND SONG ZHANG[1,2]

[1]Key Laboratory of Ministry of Education on Safe Mining of Deep Metal Mines, Northeastern University, Shenyang 110819, P. R. China
[2]Institute for Geoinformatics & Digital Mine Research, Northeastern University, Shenyang 110819, P. R. China
[3]School of Geosciences, University of South Florida, Tampa, FL 33620 USA

Corresponding author: Baodong Ma (mabaodong_rs@126.com)

This was supported in part by the National Natural Science Foundation of China under Grant 41201359 for Baodong Ma, in part by the Fundamental Research Funds for the Central Universities under Grant N160104006 for Baodong Ma, in part by the National Basic Research Program of China under Grant 2011CB707102 for Lixin Wu, and in part by the China Scholarship Council under Grant 201406085030 for Baodong Ma.

ABSTRACT A supply of minerals is critical to socioeconomic development. However, such a supply also induces negative impacts on environment and ecology, e.g., leading to dust emission and deposition. An ultra-low-grade magnetite has been exploited as a new iron type since 2001 in China. In this paper, two Landsat images were used for monitoring foliar dust in Changhe River Mining Area, China. First, models were established to estimate foliar dust using vegetation indices (VIs) differences according to laboratory spectral measurements; normalized differenced VI was selected as an optimal VI for estimating foliar dust amount based on both field and laboratory spectral measurements (RMSE = 6.58 g/m^2), and finally, the spatial patterns of foliar dust were analyzed by using ancillary high-resolution data. The result showed that most foliar dust distributed near ore transportation roads and around mining sites and tailings ponds, which was related to ultra-low-grade characteristics of the iron ore due to large-area extraction and tailings occupation, and large-amount dust emission released from ore transportation. The remote sensing method for estimating foliar dust may be beneficial for environmental management in mining areas.

INDEX TERMS Dust estimation, landsat image, VI difference, ultra-low-grade magnetite, vegetation change.

I. INTRODUCTION

Vegetation covers approximately 70 percent of the Earth's land surface and is one of the most important components of ecosystems. It is frequently influenced by human activities [1], [2]. The mining industry plays a crucial role in supplying minerals and energy for global society [3], but it also significantly affects the growth and distribution of vegetation surrounding mining areas. In a mining area, mining activities, ore transportation, mineral processing and tailings discharge can make an effect on vegetation through direct damage and indirect environmental stress [4]–[8].

With the development of economy, global demand for steel has accelerated since 2000, and thus iron ore mining activities have become intensive accordingly [6], [9]. Brazil and Australia are currently the world's leading producers of high-grade iron ore [10]. In China, iron resource is abundant, but high-grade ores are scarce [11]. Therefore, an ultra-low-grade magnetite, with the total iron content lower than 20%, has been extracted by open-pit mining and processed massively since 2001 in Chengde, Hebei Province, China [12]–[14]. Because the ratio of concentration (the number of tons of ore required to produce 1 ton of concentrate) is too high (from 8 to 12), large amount of ore is mined and transported to processing plants by truck, and large amount of tailings is produced [15]. Thus, many environmental and ecological problems are produced including vegetation damage and dust pollution due to mining activities [14]. Knowledge about vegetation change would provide valuable insight into the climatic, edaphic, geologic, and physiographic characteristics of an area [16]. Therefore, it is necessary to monitor the vegetation condition overtime and determine what changes are taking place. For this case, fortunately, remote sensing is a very useful technology for vegetation monitoring [17]. However, while the spatial resolution of some remote sensing sensors (e.g., MODIS) is often too coarse to be suitable

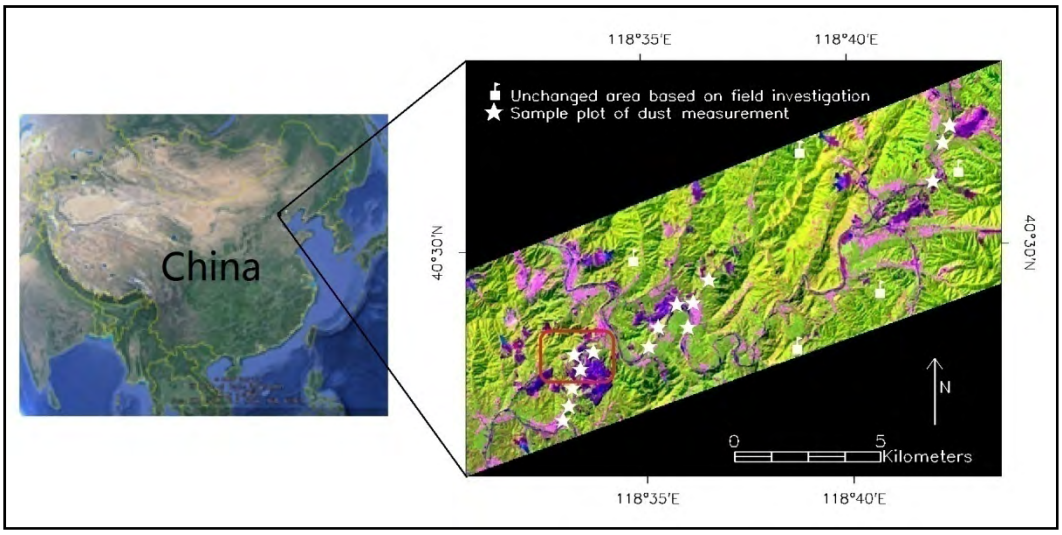

FIGURE 1. Location of the study area. Left: GoogleEarth image; Right: Landsat OLI image (bands 6, 5, 4 vs. RGB). The red box in the image shows the location of dust deposit map in Fig. 9.

for detecting vegetation change in a mining area, Landsat sensors may offer great possibilities to fill this gap with a moderate 30-m spatial resolution and long-term data record. It means that rates and spatial patterns of vegetation changes can be extracted from Landsat images. There are many successful studies on remote sensing of vegetation change in a mining area. For example, in a gold mining area, Almeida-Filho and Shimabukuro [5] used time series of Landsat TM images for mapping and monitoring vegetation degradation based on image classification techniques. It was found that the degraded areas increased firstly and then vegetation was recovered soon over mining areas after 1994. In a coal mining area, Tian *et al.* [18] used Normalized Differenced Vegetation Index (NDVI) time series to capture the fine scale vegetation changes. In some abandoned lead mines, NDVI extracted from Landsat data was used to quantify the variation of vegetation condition, and the results indicated that extensive vegetation degradation had occurred at a number of previous mining sites during the last several decades [19].

Without considering seasonal and ephemeral influences, vegetation changes can be summarized as abrupt changes and gradual changes [20]. Abrupt changes are often associated with major alterations in land cover with a significant change, whereas gradual changes are related to ''within-state'' shifts in energy response with a slight change, such as vegetation damage from insects as an abrupt change and vegetation decline from air pollution as a gradual change. Unlike abrupt changes, gradual changes are often overlooked or ignored [21]. However, there is a strong need for detecting slight vegetation change because of its important role in ecosystem management [22], [23]. Dust pollution is one of main environmental problems which can lead to a slight change of vegetation [24], [25]. Its negative effect on vegetation in urban areas has caused people's attention [26], [27]. Deposited dust on plant leaves can be used as indicators of the accumulation of inorganic pollutants along an urbanization gradient [26]. For example, to map dustfall distribution in the City of Beijing, satellite and ground based spectral data were integrated to assess dustfall weight in the city [27]. However, less attention has been paid to mining areas. Usually, dust in physical and chemical properties in a mining area is different from other areas. Therefore, the spectral response of some vegetation polluted with dust created by mining activities may be expected to be different from that in an urban area and thus some vegetation indices that might be suitable for monitoring urban vegetation change may not work for quantifying the effect of dust pollution on vegetation condition in mining areas.

Therefore, given the vegetation change in an ultra-low-grade magnetite mining area, the specific objectives of our study are to,

1) calibrate relationships between deposited dust on leaves and Vegetation Indices (VIs) in the ultra-low-degrade magnetite area based on laboratory measurements and field observations, and

2) estimate the foliar dust by using VI differencing approach for mapping foliar dust in the mining area.

II. STUDY AREA

The study area, called Changhe River Minging Area (about 134 km^2), is located in Kuancheng County, Chengde, Hebei Province, North China (see Fig. 1). It is estimated to have 2.7 billion tons of iron ore in the study area, which accounts for one third of the magnetite reserves in Hebei Province. The yearly production of iron concentrate was about 8 million tons in 2010. With a mountainous landform, the study area has an average elevation of 300 to 500 meters and is covered by dense vegetation. Changhe River is a main river

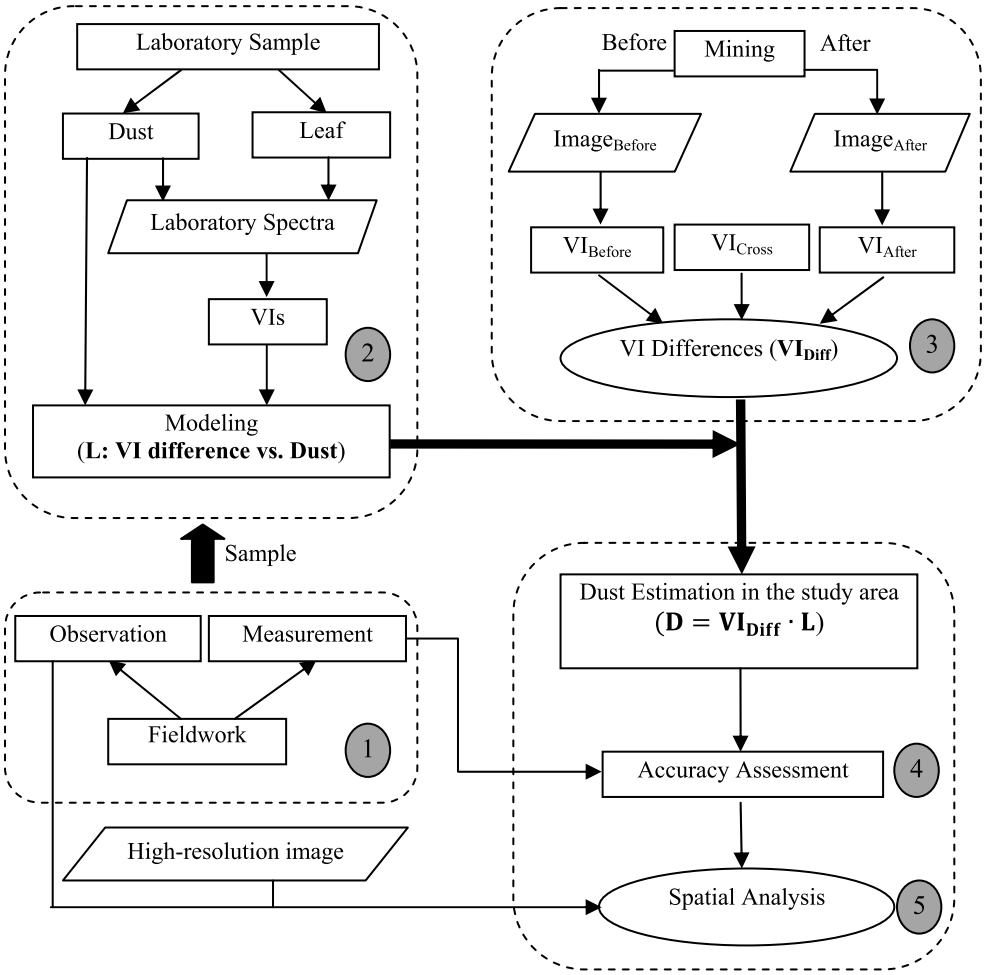

FIGURE 2. A flowchart consisting of five steps for detecting vegetation change in the mining area.

in this area. It has a continental monsoon climate with an annual precipitation of 662.5 mm and an annual temperature of 8.7°. There are several vegetation layers distributing in the study area, including arbor layer, shrub layer and herb layer. Tree species in the arbor layer mainly include *Populus cathayana, Pinus tabuliformis, Armeniaca sibirica,* and *Castanea mollissima*. There are many shrub species, such as *Vitexnegundo* var. *heterophylla, Lespedeza bicolor,* and *Ziziphusjujuba* var. *spinosagrowing* in the shrub layer, and a lot of herb species including *Bothriochloa ischaemum, Artemisia sacrorum, Commelina communis* are often seen in the herb layer.

III. MATERIALS AND METHODS

A. A WORK FLOWCHART

In order to detect vegetation change using remote sensing data in this study, five steps were taken (see Fig. 2): 1) Field work for observing *in situ* vegetation condition and measuring dust amount; 2) laboratory spectral measurement for estimating dust based on VIs; 3) Landsat image processing for analyzing VIs differences; 4) accuracy assessment and selecting VIs; and 5) estimating dust amount and analyzing its spatial patterns.

B. FIELDWORK

Types of vegetation changes were visually assessed in the field trip. The field observation data could be used to validate results of remote sensing detection for the vegetation change analysis. According to our field observation, dust emission as a major factor led to vegetation decline in the mining area. Field measurement of dust was conducted from August 5 to August 9, 2013 (see field plot locations shown in a star symbol in Fig. 1). It would be used to validate the remote sensing estimation of the dust. There was no rain during the field data sampling. Since Landsat TM and OLI data were used for dust estimation, the sampling plot size was set to 30m×30m to match the image pixel size. The 15 sampling plots were located within relatively homogenous patches with their size >50m×50m with an aid of a GPS equipment. Nine to sixteen leaves evenly located within each sampling plot were collected and washed in distilled water and then the water was dried at 70°C to obtain the dust amount. Then

TABLE 1. Summary of eight vegetation indices (VIs).

Index	Formula	References
SR	$\frac{\rho NIR}{\rho R}$	[28]
NDVI	$\frac{\rho NIR - \rho R}{\rho NIR + \rho R}$	[29]
SAVI	$\frac{(\rho NIR - \rho R)(1+L)}{(\rho NIR + \rho R + L)}$ L= 0.5 in this study.	[30]
TSAVI	$\frac{a(\rho NIR - a\rho R - b)}{a\rho NIR + \rho R - ab + X(1+a^2)}$ a=slope of the soil line, 1.2 in this study b=soil line intercept, 0.06 in this study X=adjustment factor to minimize soil noise, 0.08 in this study	[31, 36]
PVI	$\frac{1}{\sqrt{1+a^2}}(\rho NIR - a\rho R - b)$ a=slope of the soil line, 1.2 in this study b=soil line intercept, 0.06 in this study	[32]
NLI	(ρ^2NIR-ρR)/ (ρ^2NIR+ρR)	[33, 37]
MSR	$\frac{\left(\frac{\rho NIR}{\rho R}\right) - 1}{\sqrt{\frac{\rho NIR}{\rho R} + 1}}$	[34]
$TC_{greenness}$	-0.2787Blue-0.2174Green-0.5508Red +0.7221NIR+0.0773SWIR1-0.1648SWIR2	[35]

Note: ρR and ρNIR are denoted as reflectance in red (i.e., TM3, OLI4) and near-infrared (i.e., TM4, OLI5) wavelengths.

the weight of dust and the area of leaves were measured respectively to calculate the weight of dust per unit area (g/m^2) as the dust amount per pixel averagely.

C. LABORATORY EXPERIMENT FOR CALIBRATING RELATIONSHIPS BETWEEN VI DIFFERENCE AND DUST DIFFERENCE

The laboratory experiment was carried out to measure spectra from plant leaves on which varying levels of dust were applied in order to quantify a relationship between dust amount and leaf spectra. For this case, dust deposited upon leaves around a road was collected using a soft brush and then scattered on the poplar tree leaves uniformly level by level with an increment of 4 g/m^2. The dust contains 43.33% SiO_2, 16.71% CaO, 9.35% TFe, 9.30% MgO, 8.92% Al_2O_3, and 4.26% FeO. For the different levels, corresponding spectra were measured respectively with HR-1024 spectrometer (American Spectra Vista Corporation (SVC)). The SVC spectrometer covers a spectral range of 350-2500 nm with a varying spectral resolution 3.5 nm for 350-1000 nm, 9.5 nm for 1000-1890 nm, and 6.5 nm for 1890-2500 nm. Halogen lamp was selected as the light source, with an altitude angle of 60°. Then, eight commonly-used broad-band VIs were chosen and calculated to analyze their relationships with dust amount covering the leaves such that the final foliar dust difference might be spectrally estimated according to the calibrated relationships with VI differences (Table 1). Simple Ratio (SR) is the first VI designed to monitor vegetation status [28]. NDVI is the most frequently used VI without assumptions regarding land cover classes, soil type or climatic conditions [29]. Soil Adjusted Vegetation Index (SAVI) is widely used to describe dynamic soil-vegetation systems from remotely sensed data because it can minimize the influence of soil brightness [30]. Transformed Soil Adjusted Vegetation Index (TSAVI) and Perpendicular Vegetation Index (PVI) can also reduce soil background effect by considering the parameters of soil line [31], [32]. Non-Linear Index (NLI) is chosen due to its advantage in removing leaf angle distribution influence and view azimuth effect [33]. Modified Simple Ratio (MSR) is less sensitive to canopy optical and geometrical properties to assess vegetation conditions [34]. Tasselled Cap transformation greenness ($TC_{greenness}$) was designed to describe the amount of green biomass by using Landsat TM bands [35].

TABLE 2. Landsat images used for detecting the vegetation change in the study area.

Platform/Sensor	Date	Sun Azimuth	Sun Elevation	Spatial Resolution
Lansat 5/TM	August 8, 2001	129.02°	56.74°	30 m
Landsat 8/OLI	August 9, 2013	137.39°	59.70°	30 m

D. IMAGE PROCESSING AND VIs DIFFERENCING

Two scenes of Landsat TM and OLI images (path 122 and row 32) were selected for the vegetation change detection (downloaded from USGS, http://glovis.usgs.gov/). The two scenes of images were acquired on August 8, 2001 and August 9, 2013, respectively (Table 2). The two images were first geometrically registered. Then, the images were atmospherically corrected to surface reflectance by using the Fast Line-of-Slight Atmospheric Analysis of Spectral Hypercubes (FLAASH) module of ENVI software [38]. Finally the eight VIs were calculated respectively using the surface reflectance spectra retrieved from the two images.

Because the two images were acquired under different conditions (e.g., sensor difference and light condition difference), there would be differences between the two images for calculating the VIs [39]. Therefore, some unchanged areas (shown in a flag symbol in Fig. 1) based on field observation were selected to calculate the cross-image VI differences by using the following equation:

$$VI_{Cross} = VI_{OLI} - VI_{TM} \quad (1)$$

where VI_{Cross} is the VI difference value between OLI and TM images in the unchanged areas; VI_{OLI} is the VI value calculated from the OLI image; and VI_{TM} is the VI value from the TM image. The VI_{Cross} was assumed as spatially uniform on the entire image. It was used to compensate the image difference due to imaging condition differences, and thus a VI difference could be finally calculated by using following equation:

$$VI_{Diff} = VI_{After} - VI_{Before} - VI_{Cross} \quad (2)$$

where VI_{Diff} is the VI difference; VI_{Before} is the VI value before mining (i.e., calculated from 2001 TM image);

and VI_{After} is the VI value after mining (i.e., calculated from 2013 OLI image). According to image interpretation and field observation, pixels were mixed with vegetation and other features when NDVI was smaller than 0.3. To remove the effects of non-vegetated areas, pixels with NDVI < 0.3 in 2001 image were masked out in the difference image.

E. VI SELECTION

One of the main purposes for vegetation change detection in this study is to determine the dust amount in the mining area. Therefore, it is necessary to select an optimal VI that could lead to best dust estimation result. For this case, with the correlation coefficient (R) and root mean square error (RMSE) statistics as criteria, the dust estimation results created with different VI-difference-based regression models derived from the laboratory spectral measurements were compared with *in situ* measured value. Consequently, an optimal VI (with a highest R and lowest RMSE value) was selected, which would be used for detecting vegetation change in the mining area from 2001 to 2013.

F. FOLIAR DUST ESTIMATION

The spatial patterns and driving forces of vegetation change were analyzed in the study area by referring to high-resolution images, which were available through GoogleEarth as the ancillary data. They were pan-sharpened color composite images with a resolution of approximate 0.4 m, and acquired from GeoEye satellite on September 20, 2013. Using the images, we could draw boundaries of mining sites and tailings ponds and extract the fine information of ore transportation road and river in the mining area to help spatial pattern analysis.

IV. RESULTS

A. FIELD MEASUREMENT

Based on the field observation, the vegetation near an ore transportation road was significantly influenced by dust emission (see Fig. 3). In the field trip, dust was measured in the 15 sampling plots near Changfeng and Jingcheng mine sites. The maximum dust was 78.20 g/m^2.

B. RELATIONSHIPS BETWEEN FOLIAR DUST AND SPECTRA

In the laboratory experiment, the dust levels ranged from 0 to 80 g/m^2. It was observed that with increase of dust amount, the red reflectance increased and the near-infrared reflectance decreased (see Fig. 4). Furthermore, the commonly-used VIs were calculated based on the spectral measurements (see Fig. 5). The statistical results showed that all the VIs were highly correlated with dust amount, linearly or logarithmically (Table 3).

C. VI DIFFERENCES AND VI SELECTION

After the two Landsat images acquired in 2001 and 2013 were atmospherically corrected to the surface reflectance, the

FIGURE 3. Vegetation influenced by dust in the study area. a) Affected vegetation near the ore transportation road. b) Dust-covered leaves.

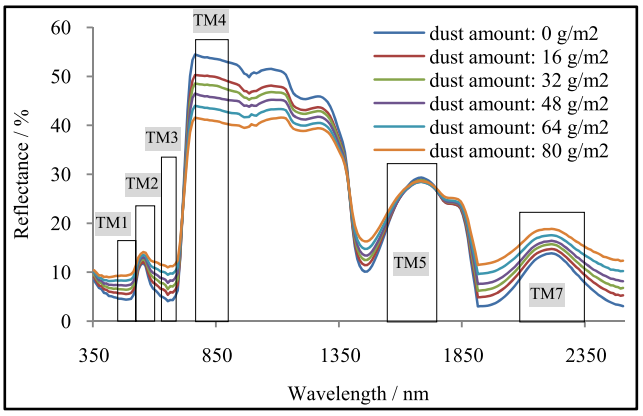

FIGURE 4. Spectra of dust-covered leaf with different dust amount.

eight VIs were calculated and VI_{Cross} was also calculated according to Equation (1). Their calculation results were summarized in Table 4.

Based on the relationships between VI differences and foliar dust difference (Table 3), the dust difference could be

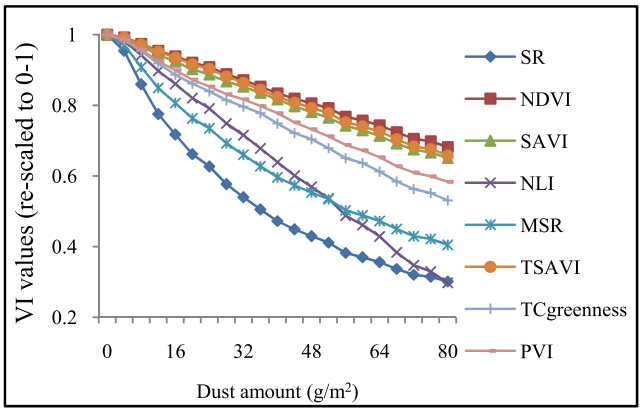

FIGURE 5. A comparison of spectral response to foliar dust variation for the eight VIs.

TABLE 3. Relationship between VI difference and foliar dust amount difference (n = 21).

Index	Relation between dust and VI		Relationship between dust difference and VI difference
	Formula	R^2	
SR	y = -65.1lnx+160.0	0.981	$\Delta y = -65.1\ln(\Delta x/xi+1)$
NDVI	y =-286.5x+244.9	0.999	$\Delta y=-286.5\Delta x$
SAVI	y = -327.3x+223.7	0.998	$\Delta y = -327.3\Delta x$
TSAVI	y = -301.5x+191.7	0.998	$\Delta y = -301.5\Delta x$
PVI	y = -610.9x+187.3	0.996	$\Delta y = -610.9\Delta x$
NLI	y = -149.1x+111.0	0.999	$\Delta y = -149.1\Delta x$
MSR	y = -87.0lnx+97.16	0.993	$\Delta y = -87.0\ln(\Delta x/xi+1)$
$TC_{greenness}$	y = -514.0x+166.8	0.996	$\Delta y = -514.0\Delta x$

Note: y is the dust amount (g/m^2) and x is the VI; Δy is the dust amount difference and Δx is the VI difference; x_i is the initial VI value.

TABLE 4. Cross-image VI difference between landsat TM and OLI sensors for the unchanged areas.

VIs	SR	NDVI	SAVI	TSAVI	PVI	NLI	MSR	$TC_{greenness}$
Mean	3.23	0.019	0.050	0.050	0.026	0.111	0.486	0.028
Standard deviation	1.89	0.025	0.033	0.034	0.018	0.074	0.284	0.020

estimated by VI differences extracted from the two image data. Before the mining activities, since dust emission had little influence on plant leaves in this study area, the dust amount was set to zero in TM image acquired in 2001. Therefore, the dust amount in OLI image acquired in 2013 could be estimated directly using following equation:

$$D = VI_{Diff} \cdot L \quad (3)$$

where D is the dust amount in the year 2013, VI_{Diff} is the VI difference between VI_{after} and VI_{before} and L is a coefficient (e.g., -286.5 g/m^2 for NDVI) derived from laboratory results in Table 3. We used the measured dust values from the 15 sampling plots to assess the accuracy of the dust amount estimated using each VI_{Diff}. The assessment results were listed in Table 5. From the table, the result showed that the dust values estimated using NDVI difference resulted in the lowest RMSE and highest R (RMSE=6.58 g/m^2, R=0.90) compared to those with the other VIs (Table 5). Therefore, NDVI was selected as an optimal VI for dust estimation.

TABLE 5. Accuracy of dust estimation based on VIs difference (n=15).

VIs	SR	NDVI	SAVI	TSAVI	PVI	NLI	MSR	$TC_{greenness}$
RMSE	19.66	6.58	15.60	17.43	16.04	28.45	58.96	19.98
R	0.57	0.90	0.48	0.64	0.37	0.54	0.71	0.28

D. FOLIAR DUST ESTIMATION IN THE MINING AREA

From the unchanged samples, the standard deviation (σ) value of NDVI difference was 0.025. For detecting unchanged and changed vegetation, the standard deviation multiplied by a constant (γ, which is from 2.5 to 3.5) is often used to determine the threshold [40]. Considering the difference of sensors, atmospheric condition and solar illumination, γ was set a value of 3.5 in this study. On the other hand, given that ultra-low-grade magnetite could not release toxic element into soil and water under non-acidic conditions [41], the dust pollution was considered as a main stress factor influencing vegetation growth. According to laboratory result, NDVI was decreased by 0.3 when the dust was 80 g/m^2. Therefore, the NDVI difference values [-0.3 to -$0.088(\gamma\sigma)$] were selected for the foliar dust estimation using Equation (3). Then the dust distribution was mapped using the NDVI difference image (see Fig. 6). The mapped result was close to the measured value (RMSE = 6.58 g/m^2, n=15) (see Fig. 7).

Information of river, road, mining site and tailings pond was extracted according to GoogleEarth-based image (see Fig. 8). The result indicated that the dusty points were located along both roadsides and around the mining sites (see Fig. 9).

V. DISCUSSION

NDVI was selected as the VI for dust estimation due to its best performance. In the study, only the poplar (*Populus cathayana*) leaves were selected to load the dust samples in the laboratory spectral measurement, which might be in favor of using NDVI. However, there still are major tree species such as *Populus cathayana, Pinus tabuliformis, Armeniaca sibirica,* and *Castanea mollissima* distributed in this study area, which are not suitable for using SAVI and TSAVI for detecting vegetation change [2]. Therefore, SAVI and TSAVI couldn't perform very well among these VIs because they are not suited for environments with various vegetation types [2]. PVI could reduce background influence on the tree canopy spectra at low vegetative covers [28]. However, vegetative coverage is generally medium to high in the study area. Thus, PVI couldn't perform very well among these VIs. Furthermore, it was found that NLI and MSR were not applicable in our study, although they are not sensitive to leaf angle distribution and canopy optical and geometrical properties. In short, NDVI was suitable for foliar dust estimation in this study because it is applicable for various vegetation species/types. This conclusion was consistent with

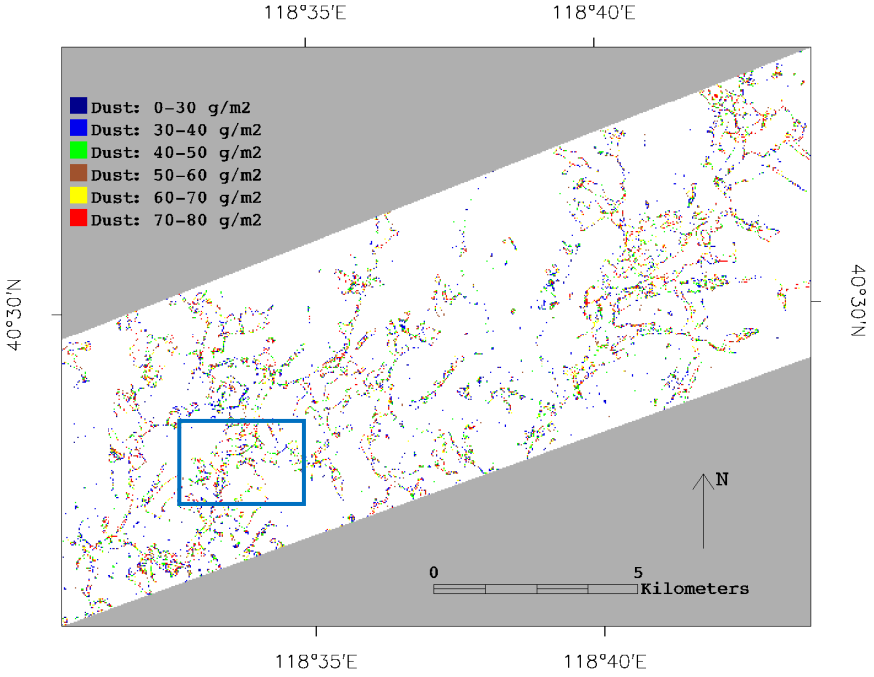

FIGURE 6. Dust mapped by NDVI difference image in the study area. The blue box in the image shows the location of dust map in Fig. 9.

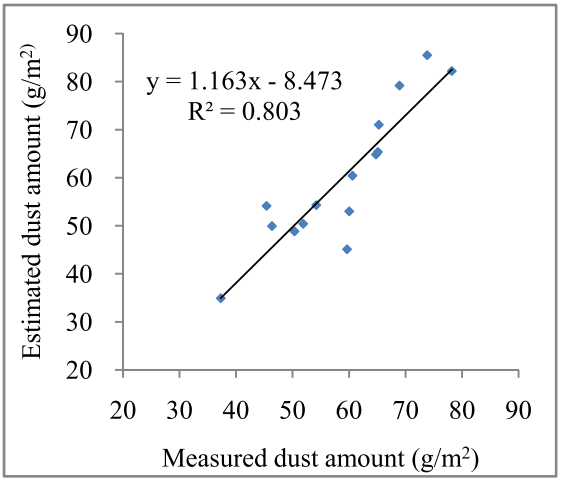

FIGURE 7. Measured foliar dust values of the 15 sampling plots against their predicted dust values using the NDVI difference estimating model.

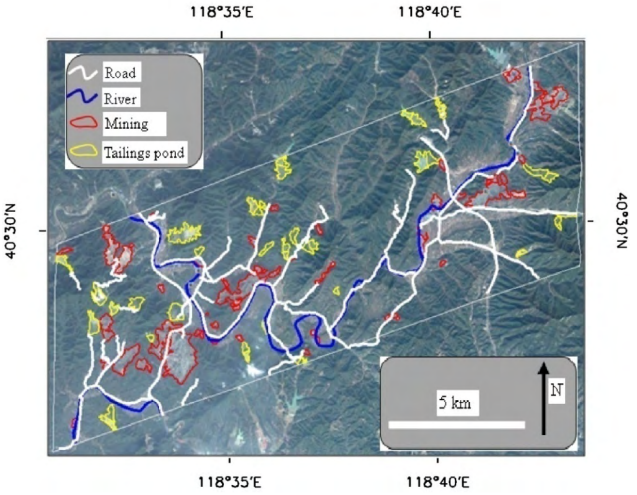

FIGURE 8. Information of river, road, mining site and tailings pond extracted from GoogleEarth image.

those drawn by other studies in which NDVI was more useful than other VIs in monitoring change of vegetation conditions [2]. In fact, NDVI was widely used for land-cover change detection [42]–[44].

When using NDVI difference to estimate dust amount in this study, the radiometric difference between the two scenes of images, caused by sensor difference and light condition difference, could be ignored. This is because the NDVI processing itself could remove or compress partial effect of atmospheric and soil, etc. on target spectra (vegetation spectra in this study), and NDVI difference could also weaken the effect of radiometric difference between the two images on the estimated result of dust using NDVI as an explanatory variable. We know that OLI sensor is different from TM sensor because their band widths are different (OLI bands with narrower band widths than TM). The light conditions were also slightly different because of the different Sun azimuth and elevation angle (Table 2). Therefore, cross-image calibration was necessary when using VI differencing approach to estimate vegetation changes. The cross-image NDVI difference (0.019) in our study was close to the result (0.0165)

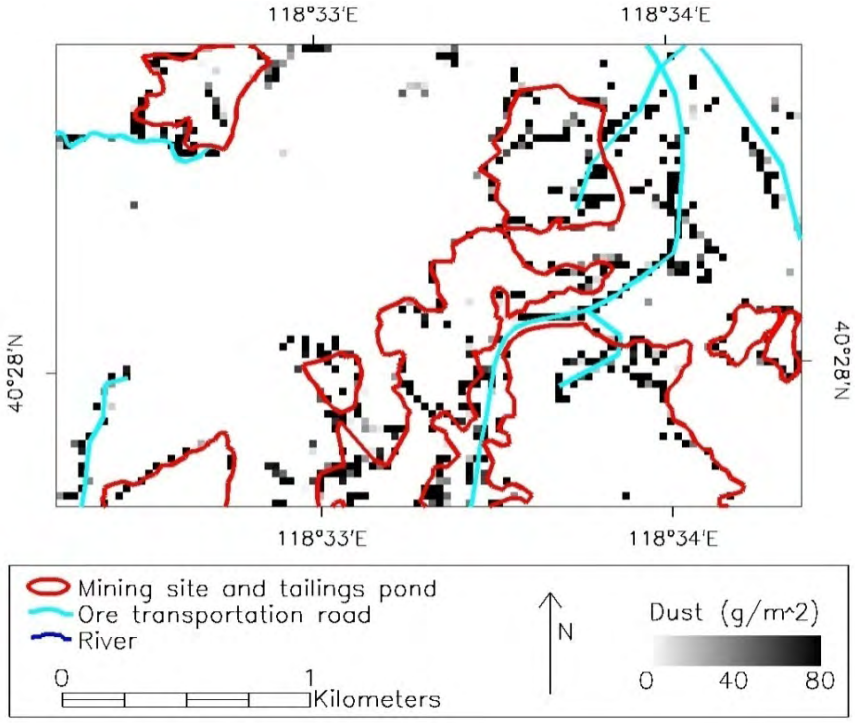

FIGURE 9. Dust mapped by NDVI difference image in the mining area.

obtained by Gong *et al.* [37] although they compared ETM+ with OLI in their study and we compared TM with OLI in our study.

Additionally, yearly NDVI might be affected by climate factors including temperature (T) and precipitation (P). In the study area, temperature would make more sense to affect NDVI [45]. Fortunately, the mean annual temperature is 8.30 °C in 2001 and 8.34 °C in 2013, while the precipitation was normal in both two years. Therefore, the NDVI difference caused by climate factors could be overlooked in this study. In case there exists a significant variation of climate factors (T, P) during the 12 years, which may lead to the NDVI change for those vegetation cover unchanged areas, our small value (0.019) of the VI_{Cross} could normalize and compensate the effect of the variation on the NDVI change. Moreover, weather condition should be considered during the data collection. Rain may scour the dust on leaves. Therefore, rainy days should be avoided to ensure the validity of data when remote sensing data and field foliar dust data are collected.

The dust emission was serious due to the frequent ore transportation by truck in the study area. For example, the annual fine iron concentration is one million tons, which means about 30 thousand tons of ore needed per day. One truck load was about 50 tons, and there were should 600 trucks for the transportation per day. The transportation derived dust emission is so intensive daily that both roadsides are filled with the dust. In our study, RMSE of dust estimation was 6.58 g/m^2. There were some reasons for the estimate error. Firstly, the relationship between NDVI difference and dust was developed in a laboratory experiment. In the experiment, we flatten the leaf for spectral measurement on the black background and we didn't consider the canopy structure factor. However, the tree leaf inclination is actually more than 0 degree. Therefore, it would contribute to error. Secondly, within a pixel area (30 m × 30 m), there might exist other components besides poplar trees, such as road surface, which could be deposited by dust. Such a pixel could be called a mixed pixel, although it might just include a small portion of other components. Thus, the estimated dust amount based on pure pixel would be different from the true value from a mixed pixel. Additionally, in fact, dust might affect the metabolic process of a leaf and then change its structure and pigments, which would have an impact on the leaf spectra [46]. However, this process was not considered in this laboratory experiment of ours.

VI. CONCLUSIONS

Based on both field and laboratory spectral measurements, foliar dust was estimated and mapped using NDVI difference approach with Landsat images in the ultra-low-grade magnetite mining area, Changhe River Mining Area, China. The result was validated and analyzed by field observations and GoogleEarth image. The main conclusions were drawn through this study as follows.

1) According to laboratory spectral measurements, models might be established to estimate foliar dust using VI differences.

2) Due to the high accuracy of dust estimation (i.e., RMSE = 6.58 g/m^2, R^2 = 0.803), NDVI might be selected to estimate dust amount using Landsat imagery. Spatial analysis results indicated that dust-covered vegetation distributed near the ore transportation roads and around mining sites and tailings ponds.

3) The ultra-low-grade magnetite exploiting needs to extract and transport massive iron ore and generates massive tailings. This ore processing would lead to heavy dust pollution, which finally results in vegetation degradation in a mining area.

In an ultra-low-grade magnetite mining area, dust emission is greater than other areas. Therefore, the study area was selected in this area. However, the method can be adopted for other areas by considering the dust sample difference.

REFERENCES

[1] P. Arellano, K. Tansey, H. Balzter, and D. S. Boyd, "Detecting the effects of hydrocarbon pollution in the Amazon forest using hyperspectral satellite images," *Environ. Pollution*, vol. 205, pp. 225–239, Oct. 2015.

[2] S. Veraverbeke, I. Gitas, T. Katagis, A. Polychronaki, B. Somers, and R. Goossens, "Assessing post-fire vegetation recovery using red–near infrared vegetation indices: Accounting for background and vegetation variability," *ISPRS J. Photogram. Remote Sens.*, vol. 68, pp. 28–39, Mar. 2012.

[3] C. J. Moran, S. Lodhia, N. C. Kunz, and D. Huisingh, "Sustainability in mining, minerals and energy: New processes, pathways and human interactions for a cautiously optimistic future," *J. Cleaner Prod.*, vol. 84, pp. 1–15, Dec. 2014.

[4] N. Demirel, M. K. Emil, and H. S. Duzgun, "Surface coal mine area monitoring using multi-temporal high-resolution satellite imagery," *Int. J. Coal Geol.*, vol. 86, no. 1, pp. 3–11, 2011.

[5] R. Almeida-Filho and Y. E. Shimabukuro, "Digital processing of a Landsat-TM time series for mapping and monitoring degraded areas caused by independent gold miners, Roraima State, Brazilian Amazon," *Remote Sens. Environ.*, vol. 79, no. 1, pp. 42–50, 2002.

[6] L. J. Sonter, D. J. Barrett, B. S. Soares-Filho, and C. J. Moran, "Global demand for steel drives extensive land-use change in Brazil's Iron Quadrangle," *Global Environ. Change*, vol. 26, pp. 63–72, May 2014.

[7] C. Mielke, N. K. Boesche, C. Rogass, H. Kaufmann, C. Gauert, and M. de Wit, "Spaceborne mine waste mineralogy monitoring in South Africa, applications for modern push-broom missions: Hyperion/OLI and EnMAP/sentinel-2," *Remote Sens.*, vol. 6, no. 8, p. 27, 2014.

[8] S. Lian, J. Ji, T. De-Jun, X. Hong-Bing, L. Zhen-Fu, and G. Bo, "Estimate of heavy metals in soil and streams using combined geochemistry and field spectroscopy in Wan-Sheng mining area, Chongqing, China," *Int. J. Appl. Earth Observat. Geoinf.*, vol. 34, pp. 1–9, Feb. 2015.

[9] M. Yellishetty, P. G. Ranjith, and A. Tharumarajah, "Iron ore and steel production trends and material flows in the world: Is this really sustainable?" *Resour., Conservation Recycling*, vol. 54, no. 12, pp. 1084–1094, 2010.

[10] M. Yellishetty and G. M. Mudd, "Substance flow analysis of steel and long term sustainability of iron ore resources in Australia, Brazil, China and India," *J. Cleaner Prod.*, vol. 84, pp. 400–410, Dec. 2014.

[11] H.-M. Li, L.-X. Li, X.-Q. Yang, and Y.-B. Cheng, "Types and geological characteristics of iron deposits in China," *J. Asian Earth Sci.*, vol. 103, pp. 2–22, May 2015.

[12] Z. Zhang *et al.*, "Spatio-temporal distribution and tectonic settings of the major iron deposits in China: An overview," *Ore Geol. Rev.*, vol. 57, pp. 247–263, Mar. 2014.

[13] S. Shuaixing, Z. Ming, T. Ming, and L. Maohe, "Recovery of phosphorite from coarse particle magnetic ore by flotation," *Int. J. Mineral Process.*, vol. 142, pp. 10–16, Sep. 2015.

[14] L. X. Li, H. M. Li, D. Z. Wang, M. J. Liu, X. Q. Yang, and J. Chen, "Ore genesis and ore-forming age of the Tiemahabaqin ultra-low-grade iron deposit in Chengde, Hebei Province, China," *Rock Mineral Anal.*, vol. 31, no. 5, pp. 898–905, 2012.

[15] L. Cui and D. Zhou, "Environmental problems caused by ultra-low-grade magnetite exploitation and countermeasures," *Resour. Environ. Eng.*, vol. 29, no. 3, p. 2, 2015.

[16] M. W. Jackson and J. R. Jensen, "An evaluation of remote sensing-derived landscape ecology metrics for reservoir shoreline environmental monitoring," *Photogramm. Eng. Remote Sens.*, vol. 71, no. 12, pp. 1387–1397, 2005.

[17] J. R. G. Townshend and C. O. Justice, "Towards operational monitoring of terrestrial systems by moderate-resolution remote sensing," *Remote Sens. Environ.*, vol. 83, no. 1, pp. 351–359, 2002.

[18] F. Tian, Y. Wang, R. Fensholt, K. Wang, L. Zhang, and Y. Huang, "Mapping and evaluation of NDVI trends from synthetic time series obtained by blending Landsat and MODIS data around a coalfield on the Loess Plateau," *Remote Sens.*, vol. 5, no. 9, p. 25, 2013.

[19] M. Kincey, L. Batty, H. Chapman, B. Gearey, S. Ainsworth, and K. Challis, "Assessing the changing condition of industrial archaeological remains on Alston Moor, UK, using multisensor remote sensing," *J. Archaeol. Sci.*, vol. 45, pp. 36–51, May 2014.

[20] J. Verbesselt, R. Hyndman, G. Newnham, and D. Culvenor, "Detecting trend and seasonal changes in satellite image time series," *Remote Sens. Environ.*, vol. 114, no. 1, pp. 106–115, 2010.

[21] J. E. Vogelmann, A. L. Gallant, H. Shi, and Z. Zhu, "Perspectives on monitoring gradual change across the continuity of Landsat sensors using time-series data," *Remote Sens. Environ.*, vol. 185, pp. 258–270, Nov. 2016.

[22] J. A. Foley *et al.*, "Amazonia revealed: Forest degradation and loss of ecosystem goods and services in the Amazon Basin," *Frontiers Ecol. Environ.*, vol. 5, no. 1, pp. 25–32, 2007.

[23] G. P. Asner, A. J. Elmore, L. P. Olander, R. E. Martin, and A. T. Harris, "Grazing systems, ecosystem responses, and global change," *Annu. Rev. Environ. Resour.*, vol. 29, pp. 261–299, Nov. 2004.

[24] M. K. Ghose and S. R. Majee, "Characteristics of hazardous airborne dust around an Indian surface coal mining area," *Environ. Monitor. Assessment*, vol. 130, nos. 1–3, pp. 17–25, 2007.

[25] J. C. Neff *et al.*, "Increasing eolian dust deposition in the western United States linked to human activity," *Nature Geosci.*, vol. 1, no. 3, pp. 189–195, 2008.

[26] E. Simon, E. Baranyai, M. Braun, C. Cserháti, I. Fábián, and B. Tóthmérész, "Elemental concentrations in deposited dust on leaves along an urbanization gradient," *Sci. Total Environ.*, vol. 490, pp. 514–520, Aug. 2014.

[27] X. Yan, W. Shi, W. Zhao, and N. Luo, "Mapping dustfall distribution in urban areas using remote sensing and ground spectral data," *Sci. Total Environ.*, vol. 506, pp. 604–612, Feb. 2015.

[28] C. F. Jordan, "Derivation of leaf-area index from quality of light on the forest floor," *Ecology*, vol. 50, no. 4, p. 4, 1969.

[29] J. W. Rouse, Jr., R. H. Haas, J. A. Schell, and D. W. Deering, "Monitoring vegetation systems in the Great Plains with ERTS," *NASA Special Publication*, vol. 351, pp. 309–317, Jan. 1974.

[30] A. R. Huete, "A soil-adjusted vegetation index (SAVI)," *Remote Sens. Environ.*, vol. 25, no. 3, pp. 295–309, 1988.

[31] F. Baret and G. Guyot, "Potentials and limits of vegetation indices for LAI and APAR assessment," *Remote Sens. Environ.*, vol. 35, no. 2, pp. 161–173, 1991.

[32] A. R. Huete, R. D. Jackson, and D. F. Post, "Spectral response of a plant canopy with different soil backgrounds," *Remote Sens. Environ.*, vol. 17, no. 1, pp. 37–53, Feb. 1985.

[33] N. S. Goel and W. Qin, "Influences of canopy architecture on relationships between various vegetation indices and LAI and FPAR: A computer simulation," *Remote Sens. Rev.*, vol. 10, no. 4, pp. 309–347, 1994.

[34] J. M. Chen, "Evaluation of vegetation indices and a modified simple ratio for boreal applications," *Can. J. Remote Sens.*, vol. 22, no. 3, pp. 229–242, 1996.

[35] J. R. Jensen, *Remote Sensing of the Environment: An Earth Resource Perspective*. Pearson Education India, Deli, India, 2009.

[36] R. Pu, "Mapping leaf area index over a mixed natural forest area in the flooding season using ground-based measurements and Landsat TM imagery," *Int. J. Remote Sens.*, vol. 33, no. 20, pp. 6600–6622, 2012.

[37] P. Gong, R. Pu, G. S. Biging, and M. R. Larrieu, "Estimation of forest leaf area index using vegetation indices derived from hyperion hyperspectral data," *IEEE Trans. Geosci. Remote Sens.*, vol. 41, no. 6, pp. 1355–1362, Jun. 2003.

[38] *FLAASH User's Guide, Atmospheric Correction Module: QUAC and FLAASH User's Guide*, ITT Visual Information Solutions, Boulder, CO, Aug. 2009, p. 44.

[39] D. P. Roy *et al.*, "Characterization of Landsat-7 to Landsat-8 reflective wavelength and normalized difference vegetation index continuity," *Remote Sens. Environ.*, vol. 185, pp. 57–70, Nov. 2016.
[40] D. Lu, P. Mausel, M. Batistella, and E. Moran, "Land-cover binary change detection methods for use in the moist tropical region of the Amazon: A comparative study," *Int. J. Remote Sens.*, vol. 26, no. 1, pp. 101–114, Jan. 2005.
[41] K. N. Kuki, M. A. Oliva, E. G. Pereira, A. C. Costa, and J. Cambraia, "Effects of simulated deposition of acid mist and iron ore particulate matter on photosynthesis and the generation of oxidative stress in Schinus terebinthifolius Radii and Sophora Tomentosa L," *Sci. Total Environ.*, vol. 403, no. 1, pp. 207–214, 2008.
[42] R. Pu, P. Gong, Y. Tian, X. Miao, R. Carruthers, and G. Anderson, "Using classification and NDVI differencing methods for monitoring sparse vegetation coverage: A case study of saltcedar in Nevada, USA," *Int. J. Remote Sens.*, vol. 29, no. 14, pp. 3987–4011, 2008.
[43] C. He, Y. Zhao, J. Tian, P. Shi, and Q. Huang, "Improving change vector analysis by cross-correlogram spectral matching for accurate detection of land-cover conversion," *Int. J. Remote Sens.*, vol. 34, no. 4, pp. 1127–1145, 2013.
[44] X. Chen, D. Yang, J. Chen, and X. Cao, "An improved automated land cover updating approach by integrating with downscaled NDVI time series data," *Remote Sens. Lett.*, vol. 6, no. 1, pp. 29–38, 2015.
[45] Y. Wu, N. Li, and J. Yuan, "NDVI changes and their relation with climate factors in Chengde based on SPOT-VGT," *Chin. Agricult. Sci. Bull.*, vol. 27, no. 11, p. 041, 2011.
[46] G. Borka, "Effect of metalliferous dusts from dressing works on the growth, development, main metabolic processes and yields of winter wheat *in situ* and under controlled conditions," *Environ. Pollution Ser. A, Ecol. Biol.*, vol. 35, no. 1, pp. 67–73, 1984.

BAODONG MA received the B.S. degree in surveying engineering from Central South University, China, in 2001 and the M.S. and Ph.D. degrees in digital mine engineering from Northeastern University, China, in 2008 and 2014, respectively.

Since 2008, he has been a Lecturer with the Surveying Engineering Department, Northeastern University, China. He has authored over 20 articles. His research interests include hyperspectral remote sensing of vegetation, and remote sensing monitoring for environment in mining areas.

RUILIANG PU received the Ph.D. degree in cartography and geographic information system, conducted at the Department of Environmental Science, Policy, and Management, UC Berkeley, from the Chinese Academy of Sciences, in 2000.

He is currently an Associate Professor with the School of Geosciences, University of South Florida. His current research interests are in mapping and characterizing seagrass habitats using spacecraft observations, urban environmental studies, and urban tree canopy mapping/species identification using thermal and high-resolution satellite imagery.

LIXIN WU received the B.S. degree in mining survey from the China University of Mining and Technology, Xuzhou, China, in 1988, and the M.S. and Ph.D. degrees in geomatics from the China University of Mining and Technology, Beijing, China, in 1991 and 1997, respectively.

He has been with Northeastern University, Shenyang, China, as a Changjiang Awarded Professor and the Head of the Institute for Geo-informatics and Digital Mine Research. His research interests include geohazards synergic observation, remote sensing rock mechanic, and geospatial informatics.

Dr. Wu was the Co-Chair of the User Applications in Remote Sensing Committee, the IEEE Geoscience and Remote Sensing Society. He is currently a member of the Infrastructure Implementation Board of Group on Earth Observation, the Vice Chairman of Space Observation Committee of the China Seismology Society, and the Editor-in-Chief of the *Journal of Geography and Geo-Information Science* (Chinese).

SONG ZHANG received the B.S. degree in surveying engineering from Liaoning Technical University, China, in 2015. He is currently pursuing the M.S. degree in survey engineering with Northeastern University, China.

His research interests include hyperspectral remote sensing of vegetation and environmental monitoring in mining areas.